

# $W^+W^- + 3\text{-jet}$ production at the Large Hadron Collider in next-to-leading-order QCD

F. Febres Cordero, P. Hofmann, and H. Ita

*Physikalisches Institut, Albert-Ludwigs-Universität Freiburg, D-79104 Freiburg, Germany*

(Received 12 January 2016; published 8 February 2017)

We present next-to-leading-order (NLO) QCD predictions to  $W^+W^-$  production in association with up to three jets at hadron colliders. We include contributions from couplings of the  $W$  bosons to light quarks as well as trilinear vector couplings. These processes are used in vector-boson coupling measurements, are background to Higgs signals and are needed to constrain many new physics scenarios. For the first time NLO QCD predictions are shown for electroweak di-vector boson production with three jets at a hadron collider. We show total and differential cross sections for the LHC with proton center-of-mass energies of 8 and 13 TeV. To perform the calculation we employ on-shell and unitarity methods implemented in the BlackHat library along with the SHERPA package. We have produced event files that can be accessed for future dedicated studies.

DOI: 10.1103/PhysRevD.95.034006

The increasing energy reach of the Large Hadron Collider (LHC) and the large data sets expected from the ATLAS and CMS experiments widen the need for precise theoretical predictions. Scattering processes including final-state leptons, produced through intermediate electroweak vector bosons ( $W^\pm$ ,  $Z$  or  $\gamma$ ), with multiple jets are particularly important as they probe the electroweak sector of the Standard Model (SM) and are central to many searches for new particles. Precise theory predictions are necessary in order to challenge the SM and also to extend the experiments' reach by providing a reference for backgrounds to rare events. Here, we study high-multiplicity signatures which open new perspectives on fundamental interactions. They can arise when several particles recoil against the core scattering processes, exposing the dynamics of fundamental interactions. Furthermore, such signatures can be the outcome of decay chains of potential new heavy particles. The comparison of precise theoretical predictions to experimental measurements will open numerous ways to sharpen our understanding of physics at the TeV scale.

The production of two oppositely charged  $W$  bosons in association to several jets stands out due to its rich phenomenology. This final-state configuration is obtained in top-quark pair production, as the top quarks decay into bottom quarks and  $W$  bosons. It also appears in the weak vector-boson-fusion (VBF) mechanism, in which scattering quarks emit intermediate vector bosons which scatter and eventually produce a  $W^+W^-$  pair. The VBF production mode of the Higgs boson which decays to  $W$  bosons contributed to early limits of the Higgs-boson mass [1] and helped the measurement of its couplings and spin [2]. The distinguishing signature of these VBF processes are two forward pointing jets (arising from the emitter quarks) including a radiation gap between the jets. Precise predictions for  $W^+W^- + 3\text{-jet}$  production allow us to explore

this gap in detail. Moreover, predictions for  $W^+W^- + n$  jet processes are important for measuring trilinear and quartic vector-boson couplings. Finally, in many scenarios of physics beyond the SM these leptonic states appear in combination with many jets as end products of decay chains of heavy colored particles.

In this paper, we present NLO QCD predictions for  $W^+W^- + 3\text{-jet}$  production, which is the first time this level of precision is achieved for processes of electroweak di-vector boson production in association with three jets. Results for  $W^+W^- + n$ -jet production with  $n = 0, 1$  and  $2$  are shown as well. We include contributions from couplings of the vector bosons to light quarks (omitting top contributions) as well as trilinear vector couplings. We consider the leading electroweak contributions. A phenomenological study is presented to assess the impact of NLO QCD corrections on the total and differential cross sections at the LHC with collision energies of 8 and 13 TeV. The reliability of the theory predictions is significantly improved by including QCD corrections, as scale uncertainties for  $W^+W^- + 3$  jet total cross sections are reduced from 40% at leading order (LO) to about 5% at NLO.

Measurements of the  $WW + n$ -jet production cross section ( $n \geq 0$ ) have a long history at hadron colliders. The inclusive  $WW$  cross section was measured first by the CDF [3] and D0 [4] experiments at the Tevatron, and recently by the ATLAS [5,6] and CMS [7,8] experiments at the LHC. Very recently a first dedicated measurement of the cross sections for  $W^+W^-$  production in association with 0, 1 and 2 jets has been published [9] by the CDF experiment. In the context of the exploration of the electroweak sector, many studies have been carried out to measure (and in cases subtract) direct  $WW + n$  jet signals. For example,  $W^+W^- + n$ -jet production has been thoroughly studied in order to reduce its contributions (through kinematic constraints and jet vetoes) as

background for Higgs-boson studies in the  $W^+W^-$  decay mode [10–13]. A year ago both ATLAS [14] and CMS [15] showed first evidence for the production of same charge vector-boson scattering. In the future dedicated studies at the LHC of  $W^+W^- +$  jets production in bins of jet multiplicity should be carried out, in order to assist measurements of Higgs-boson properties and couplings of massive vector bosons. It is the aim of this work to provide reliable SM predictions for such a task.

The importance of precise theoretical predictions for inclusive  $W^+W^-$  pair production has stimulated many developments starting from the early LO results [16], including NLO QCD corrections [17] and, very recently, the first next-to-next-to-leading (NNLO) order QCD prediction [18]. For  $W^+W^-$  pair production in association with jets, NLO QCD predictions are available for one [19] and two jets [20–22] (including same sign studies in Ref. [23]). NLO QCD corrections are particularly large at low jet multiplicity due to the opening of additional partonic channels and the release of kinematic constraints. In general, the QCD corrections significantly reduce the unphysical factorization- and renormalization-scale dependence, and provide then the first quantitatively reliable predictions for total cross sections and shapes of distributions.

The virtual corrections to  $W^+W^- + 3$ -jet production involve up to five final-state objects. Counting the leptonic decay products of the weak vector bosons, this process contains a phase space with up to seven partonic/leptonic final states. This is a state-of-the-art NLO QCD calculation for processes with five or more objects in the final state [24–27]. We employ the BlackHat library [28] to compute the one-loop matrix elements. This library has been developed based on on-shell methods [29–33] that rely on the unitarity and factorization properties of scattering amplitudes to construct loop and tree amplitudes. Such methods are efficient and scale well as the number of external legs increases. In particular the BlackHat library has produced NLO QCD predictions to vector-boson production in association with up to five jets [24–26,34–37], pure 4 jet production [38] and di-photon production in association with 2 jets [39].

In this work we extended the functionality of the BlackHat library to provide virtual matrix elements for QCD corrections to two massive vector bosons and up to five partons (gluons or quarks). To this end on-shell recursion relations [31] for tree amplitudes of quarks, gluons and massive vector bosons [40] (including decay products) have been provided. As a cross check, we implemented the same tree amplitudes through off-shell recursions [41]. Both implementations have been compared yielding numerically identical results. In addition, we provided infrastructure to compute loop amplitudes based on the new tree input. Finally, tree and loop amplitudes are assembled in an automated way [42] into the virtual, squared matrix elements.

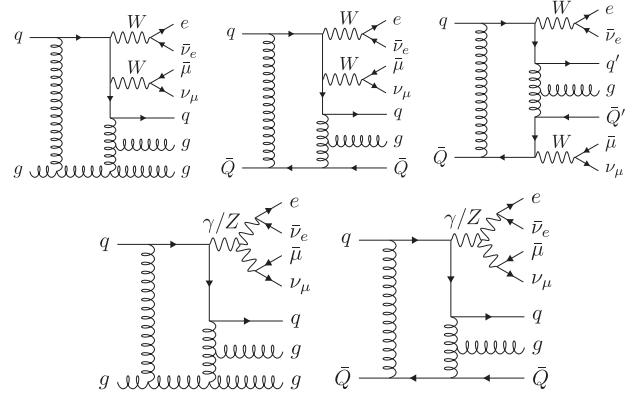


FIG. 1. Sample diagrams of loop amplitudes for  $gg \rightarrow W^+W^-q^{(l)}gg$  and  $q\bar{Q} \rightarrow W^+W^-q^{(l)}g\bar{Q}^{(l)}$ , followed by  $W^- \rightarrow e\bar{\nu}_e$  and  $W^+ \rightarrow \mu\bar{\nu}_\mu$ .

We show representative virtual diagrams in Fig. 1. We use a leading-color approximation in the finite virtual contributions [42], including virtual quark loops, but dropping other subleading color terms in the partial loop amplitudes. We keep the full color dependence in born and real radiation contributions. We have confirmed that this approximation is an excellent one for  $W^+W^- + 1, 2$  jet production, shifting the total cross section below 1%, less than uncertainties from parton distributions or higher-order terms in  $\alpha_s$ . The omitted contributions correspond to  $N_c$ -suppressed gluon-loop diagrams and diagrams with vector bosons coupled directly to closed quark loops, as well as diagrams with a massive top quark in the loop. In fact, the latter two contributions have been shown to shift the total cross section below the percent level [21]. We therefore expect the omitted subleading color corrections to  $W^+W^- + 3$ -jet production to be small.

We consider the double resonant contributions and include the full Breit-Wigner distribution for intermediate  $Z$  and  $W$  bosons; decays to leptons retain all spin correlations. We consider a diagonal Cabibbo-Kobayashi-Maskawa (CKM) matrix, and for loop diagrams we consider five light quark flavors;  $n_f = 5$ . Except for canceling infrared collinear poles, we do not include contributions from external bottom quarks; bottom final states are vetoed being naturally attributed to studies of top production which we do not consider here. Given the subleading nature of bottom parton-distribution functions (PDFs), di-bottom initial states are small contributing at the percent level [19] at low multiplicities justifying the approach.

The remaining NLO ingredients, the real-emission and dipole-subtraction terms [43], are computed by COMIX [44], part of the SHERPA package [45]. We also use SHERPA to perform phase-space integration. We store intermediate results in public root-format [46] ntuple files [47], recording parton momenta, along with the information on scale-, coupling- and PDF-dependent contributions to the event weights. The effects of varying scale and input parameters

as well as tightening of phase-space cuts are obtained efficiently using the ntuple files without recomputing the time-consuming matrix elements.

The results have been checked by observing the explicit cancellation of infrared poles and comparison of one-loop matrix elements at individual phase-space points where available [48], as well as comparison to an implementation using off-shell recursion relations [41]. The SHERPA implementation of the real-emission and dipole-subtraction terms has a dependence on an arbitrary parameter  $\alpha_{\text{dipole}}$  [49], and we have made dedicated studies to show that our results are independent of it.

In our study, we consider the inclusive processes  $pp \rightarrow W^+W^- + n \text{ jets}$  ( $n = 0, 1, 2$  and  $3$ , and also  $n = 4$  at LO) at the LHC with proton center-of-mass energy of  $\sqrt{s} = 8$  and  $13$  TeV. The  $W$  bosons are decayed into oppositely charged light lepton-neutrino pairs; we require an electron as well as an anti-muon. We consider leptons from distinct flavors to distinguish from processes with pairs of  $Z$  bosons,  $pp \rightarrow ZZ(\rightarrow \ell^+\ell^-\nu\bar{\nu}) + \text{jets}$ . We set dynamically the renormalization and factorization scales according to  $\mu = \mu_r = \mu_f = \hat{H}_T/2$ , where  $\hat{H}_T = \sum_j p_T^j$  and the sum runs over all final-state partons and leptons labeled by  $j$ . Scale-dependence bands are constructed from the minimum and maximum of the given observable evaluated at five values:  $\mu/2, \mu/\sqrt{2}, \mu, \sqrt{2}\mu, 2\mu$ . The following phase space cuts are applied:  $p_T^{e,\mu} > 20$  GeV,  $|\eta^{e,\mu}| < 2.4$ ,  $E_T > 30$  GeV,  $p_T^{e\mu} > 30$  GeV and  $m_{e\mu} > 10$  GeV. Jets are defined with the anti- $k_T$  jet algorithm [50] with  $R = 0.4$  and requiring  $p_T^{\text{jet}} > 30$  GeV,  $|\eta^{\text{jet}}| < 4.5$ , and are ordered in  $p_T$ . Here,  $p_T$  are transverse momenta;  $\eta$ , pseudo rapidities;  $m_{e\mu}$ , and  $p_T^{e\mu}$  the mass and transverse momentum of the electron-muon system, respectively. We identify  $E_T$  with the magnitude of the sum of the momenta of the neutrinos in the transverse plane. At NLO we use the MSTW2008nlo [51] PDFs and the MSTW2008lo set at LO, and we set  $\alpha_s$  consistently as provided by the PDFs. The  $W$  and  $Z$  boson mass and width are given, respectively, by  $\Gamma_W = 2.085$  GeV,  $M_W = 80.399$  GeV and  $\Gamma_Z = 2.4952$  GeV,  $M_Z = 91.188$  GeV. We use the complex-mass

scheme [52] in order to treat the unstable vector bosons in a gauge invariant way.

In Table I, we present LO and NLO parton-level cross sections at  $\sqrt{s} = 8$  and  $13$  TeV for inclusive  $W^+W^-$  production accompanied by zero through three jets. In addition we show LO results for  $W^+W^- + 4$  jets. The scale-variation for the NLO cross sections amount to 5% for our setup as opposed to the LO values which vary from 7% to 50% for zero up to four jets at  $13$  TeV. We also display the “jet-production” ratios of  $W^+W^- + n$  jet to  $W^+W^- + (n - 1)$ -jet production. These kinds of ratios are less sensitive to experimental and theoretical systematics than the absolute cross sections. Despite a significant dependence of the ratios on the phase-space cuts imposed [53], universal behavior of these ratios is expected for large jet multiplicities. More detailed studies of these ratios for higher jet multiplicities at NLO shall be performed.

As expected total cross sections increase with the center-of-mass energy (see Table I). As phase-space cuts are maintained, the increase in center-of-mass energy opens more phase-space volume and enlarges the range of momentum fractions of partons sampled in the incoming protons. We observe that the jet ratios of  $W^+W^- + n$  jet production increase with the collision energy consistent with the fact that additional jets have more phase space available.

In Fig. 2, we show the  $p_T$  spectra of the leading three jets in  $W^+W^- + 3$ -jet production at LO and NLO at  $\sqrt{s} = 13$  TeV; in the lower panels we normalize (bin-by-bin) to the NLO prediction and show scale-dependence bands. We observe a noticeable shape difference between the LO and NLO distributions for the first two leading jets, while the shape for the third jet distribution is very similar at LO and NLO. This behavior has been observed in  $W$  production in association with jets [24]. Figure 3 shows the distribution of the total hadronic transverse energy  $H_T^{\text{had}} = \sum_j E_{T,j}^{\text{jet}}$ . We show the NLO and LO predictions, along with their scale-dependence bands. As in the  $p_T$  distributions, the NLO band is narrower. The shapes of the distributions at LO and NLO are similar, although they differ in their normalization.

TABLE I. Total cross sections in femtobarns (fb) for  $W^+W^- + n$ -jet production at the LHC with  $\sqrt{s} = 8$  and  $13$  TeV. We show parton level LO and NLO QCD results, as well as the corresponding jet cross section ratios,  $R_n = (W^+W^- + n \text{ jet})/(W^+W^- + (n - 1) \text{ jet})$ . The NLO result for  $W^+W^- + 3$  jets uses the leading-color approximation discussed in the text. In parentheses we show the numerical integration error, and the dependence on the unphysical renormalization and factorization scales is quoted in superscripts and subscripts.

$n$	$W^+W^- + n \text{ jet}$ (8 TeV)		$R_n$ (8 TeV)		$W^+W^- + n \text{ jet}$ (13 TeV)		$R_n$ (13 TeV)	
	LO	NLO	LO	NLO	LO	NLO	LO	NLO
0	142.2(3) <sup>+3.7</sup> <sub>-5.3</sub>	207.4(7) <sup>+5.1</sup> <sub>-3.3</sub>	...	...	230.7(5) <sup>+13.7</sup> <sub>-16.7</sub>	358(2) <sup>+7.3</sup> <sub>-4.5</sub>	...	...
1	60.9(1) <sup>+9.8</sup> <sub>-8.0</sub>	76.0(2) <sup>+3.6</sup> <sub>-3.9</sub>	0.428(1)	0.366(2)	131.6(2) <sup>+16.3</sup> <sub>-14.0</sub>	165.1(6) <sup>+7.2</sup> <sub>-7.1</sub>	0.571(2)	0.462(3)
2	29.43(6) <sup>+9.99</sup> <sub>-6.91</sub>	28.5(1) <sup>+0.4</sup> <sub>-1.8</sub>	0.483(1)	0.376(2)	77.5(2) <sup>+23.1</sup> <sub>-16.6</sub>	72.7(4) <sup>+0.2</sup> <sub>-3.2</sub>	0.589(2)	0.440(3)
3	11.11(2) <sup>+5.73</sup> <sub>-3.51</sub>	9.05(12) <sup>+0.08</sup> <sub>-0.90</sub>	0.378(1)	0.317(5)	35.59(6) <sup>+16.66</sup> <sub>-10.55</sub>	28.1(3) <sup>+0.0</sup> <sub>-2.1</sub>	0.459(1)	0.386(5)
4	3.58(1) <sup>+2.49</sup> <sub>-1.37</sub>	...	0.322(1)	...	14.12(8) <sup>+9.05</sup> <sub>-5.14</sub>	...	0.397(2)	...

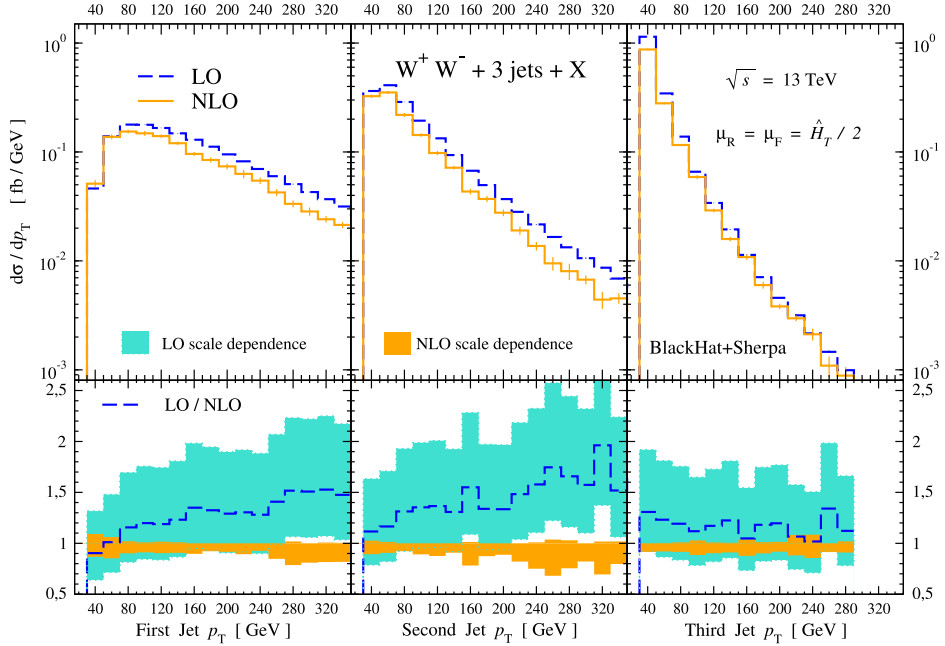


FIG. 2. A comparison of the  $p_T$  distributions of the leading three jets in  $W^+W^- + 3$ -jet production at the LHC at  $\sqrt{s} = 13$  TeV. In the upper panels the NLO distribution is the solid (orange) histogram, and the LO predictions are shown as dashed (blue) lines. The thin vertical line in the center of each bin (where visible) gives its numerical (Monte Carlo) integration error. The lower panels show the LO distribution and LO and NLO scale-dependence bands normalized to the central NLO prediction. The bands are shaded (orange) for NLO and light-shaded (cyan) for LO.

With our new matrix elements for di-vector bosons production, a number of future directions for studies open up. In order to compare the parton-level predictions to experimental data, nonperturbative effects (such as hadronization and the underlying event) have to be estimated. NLO parton-shower Monte Carlo programs [54] achieve

this task. The virtual corrections computed here can be incorporated into such studies. Initially, cross section ratios, like the ones presented in Table I, can provide useful predictions for direct comparison to data, as parton-shower and nonperturbative effects are largely canceled in them. Furthermore, the results of this study show a good control over predictions to  $W^+W^- + 3$ -jet production within the SM. A number of immediate phenomenological questions can be addressed. It will be interesting, and necessary, to explore the effect of QCD corrections for distinguished phase space regions requiring two forward tagging jets which emphasize weak vector-boson-fusion event topologies as well as cuts for new physics searches.

The presented scattering process is but the first step toward providing a new class of predictions. Beyond  $W^+W^- + n$  jet processes, additional combinations of vector-boson pairs  $VV'$  (with  $V$  and  $V'$  either  $W^\pm$ ,  $Z$  or a photon) as well as interference effects with signal processes play an important role for exploring the electroweak symmetry breaking mechanism. These processes are well within reach of the current BlackHat library, and we expect to provide precise theory predictions in the near future.

## ACKNOWLEDGMENTS

We thank Z. Bern, L. J. Dixon, S. Höche, D. A. Kosower, D. Maitre and C. Schwinn for helpful discussions. H. I.'s work is supported by a Marie Skłodowska-Curie Action Career-Integration Grant No. PCIG12-GA-2012-334228 of

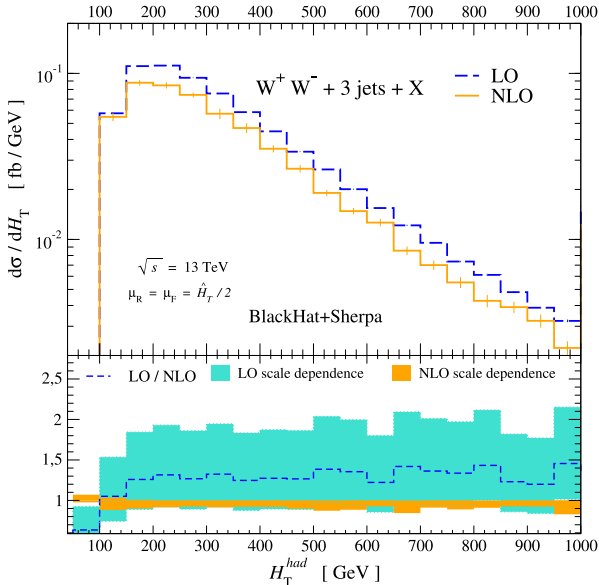


FIG. 3. The  $H_T^{\text{had}}$  distribution for  $W^+W^- + 3$  jets at  $\sqrt{s} = 13$  TeV.

the European Union. P. H.'s work is supported by the Junior Professor Program of Ministry of Science, Research and the Arts of the state of Baden-Württemberg, Germany. The work of F.F.C. is supported by the Alexander von Humboldt Foundation, in the framework of the Sofja Kovalevskaja Award 2014, endowed by the German

Federal Ministry of Education and Research. This work was performed on the bwUniCluster funded by the Ministry of Science, Research and the Arts Baden-Württemberg and the Universities of the State of Baden-Württemberg, Germany, within the framework program bwHP.

- 
- [1] G. Aad *et al.* (ATLAS Collaboration), *Phys. Rev. Lett.* **108**, 111802 (2012); **716**, 62 (2012); S. Chatrchyan *et al.* (CMS Collaboration), *Phys. Lett. B* **710**, 91 (2012).
- [2] G. Aad *et al.* (ATLAS Collaboration), *Phys. Lett. B* **726**, 88 (2013); **734**, 406 (2014); **726**, 120 (2013); S. Chatrchyan *et al.* (CMS Collaboration), *J. High Energy Phys.* 01 (2014) 096.
- [3] T. Aaltonen *et al.* (CDF Collaboration), *Phys. Rev. Lett.* **104**, 201801 (2010).
- [4] V. Abazov *et al.* (D0 Collaboration), *Phys. Rev. Lett.* **103**, 191801 (2009).
- [5] G. Aad *et al.* (ATLAS Collaboration), *Phys. Rev. Lett.* **107**, 041802 (2011).
- [6] G. Aad *et al.* (ATLAS Collaboration), *Phys. Rev. D* **87**, 112001 (2013); **88**, 079906 (2013).
- [7] S. Chatrchyan *et al.* (CMS Collaboration), *Eur. Phys. J. C* **73**, 2610 (2013).
- [8] S. Chatrchyan *et al.* (CMS Collaboration), *Phys. Lett. B* **721**, 190 (2013).
- [9] T. A. Aaltonen *et al.* (CDF Collaboration), *Phys. Rev. D* **91**, 111101 (2015); **92**, 039901 (2015).
- [10] T. Aaltonen *et al.* (CDF Collaboration), *Phys. Rev. D* **88**, 052012 (2013).
- [11] V. M. Abazov *et al.* (D0 Collaboration), *Phys. Rev. D* **88**, 052006 (2013).
- [12] S. Chatrchyan *et al.* (CMS Collaboration), *J. High Energy Phys.* 01 (2014) 096.
- [13] G. Aad *et al.* (ATLAS Collaboration), *Phys. Rev. D* **92**, 012006 (2015).
- [14] G. Aad *et al.* (ATLAS Collaboration), *Phys. Rev. Lett.* **113**, 141803 (2014).
- [15] V. Khachatryan *et al.* (CMS Collaboration), *Phys. Rev. Lett.* **114**, 051801 (2015).
- [16] R. W. Brown and K. O. Mikaelian, *Phys. Rev. D* **19**, 922 (1979).
- [17] J. Ohnemus, *Phys. Rev. D* **44**, 1403 (1991); S. Frixione, *Nucl. Phys.* **B410**, 280 (1993); L. J. Dixon, Z. Kunszt, and A. Signer, *Nucl. Phys.* **B531** (1998) 3; J. M. Campbell and R. K. Ellis, *Phys. Rev. D* **60**, 113006 (1999); L. J. Dixon, Z. Kunszt, and A. Signer, *Phys. Rev. D* **60**, 114037 (1999); J. M. Campbell, R. K. Ellis, and C. Williams, *J. High Energy Phys.* 07 (2011) 018.
- [18] T. Gehrmann, M. Grazzini, S. Kallweit, P. Maierhöfer, A. von Manteuffel, S. Pozzorini, D. Rathlev, and L. Tancredi, *Phys. Rev. Lett.* **113**, 212001 (2014).
- [19] J. M. Campbell, R. K. Ellis, and G. Zanderighi, *J. High Energy Phys.* 12 (2007) 056; S. Dittmaier, S. Kallweit, and P. Uwer, *Phys. Rev. Lett.* **100**, 062003 (2008); *Nucl. Phys. B* **826**, 18 (2010); F. Cascioli, S. Höche, F. Krauss, P. Maierhöfer, S. Pozzorini, and F. Siegert, *J. High Energy Phys.* 01 (2014) 046; J. M. Campbell, D. J. Miller, and T. Robens, *Phys. Rev. D* **92**, 014033 (2015).
- [20] T. Melia, K. Melnikov, R. Rontsch, and G. Zanderighi, *Phys. Rev. D* **83**, 114043 (2011).
- [21] N. Greiner, G. Heinrich, P. Mastrolia, G. Ossola, T. Reiter, and F. Tramontano, *Phys. Lett. B* **713**, 277 (2012).
- [22] J. Alwall, R. Frederix, S. Frixione, V. Hirschi, F. Maltoni, O. Mattelaer, H.-S. Shao, T. Stelzer, P. Torrielli, and M. Zaro, *J. High Energy Phys.* 07 (2014) 079.
- [23] T. Melia, K. Melnikov, R. Rontsch, and G. Zanderighi, *J. High Energy Phys.* **12** (2010) 053; F. Campanario, M. Kerner, L. D. Ninh, and D. Zeppenfeld, *Phys. Rev. D* **89**, 054009 (2014).
- [24] Z. Bern, L. J. Dixon, F. F. Cordero, S. Höche, H. Ita, D. A. Kosower, D. Matre, and K. J. Ozeren, *Phys. Rev. D* **88**, 014025 (2013).
- [25] C. F. Berger, Z. Bern, L. J. Dixon, F. F. Cordero, D. Forde, T. Gleisberg, H. Ita, D. A. Kosower, and D. Maître, *Phys. Rev. Lett.* **106**, 092001 (2011).
- [26] H. Ita, Z. Bern, L. J. Dixon, F. F. Cordero, D. A. Kosower, and D. Maître, *Phys. Rev. D* **85**, 031501 (2012).
- [27] S. Badger, B. Biedermann, P. Uwer, and V. Yundin, *Phys. Rev. D* **89**, 034019 (2014); S. Badger, A. Guffanti, and V. Yundin, *J. High Energy Phys.* 03 (2014) 122; A. Denner and R. Feger, *J. High Energy Phys.* 11 (2015) 209; G. Bevilacqua, H. B. Hartanto, M. Kraus, and M. Worek, *Phys. Rev. Lett.* **116**, 052003 (2016).
- [28] C. F. Berger, Z. Bern, L. J. Dixon, F. F. Cordero, D. Forde, H. Ita, D. A. Kosower, and D. Maître, *Phys. Rev. D* **78**, 036003 (2008).
- [29] Z. Bern, L. J. Dixon, D. C. Dunbar, and D. A. Kosower, *Nucl. Phys.* **B425**, 217 (1994); **B435**, 59 (1995); Z. Bern, L. J. Dixon, and D. A. Kosower, *Nucl. Phys.* **B513**, 3 (1998).
- [30] R. Britto, F. Cachazo, and B. Feng, *Nucl. Phys.* **B725**, 275 (2005).
- [31] R. Britto, F. Cachazo, B. Feng, and E. Witten, *Phys. Rev. Lett.* **94** (2005) 181602.
- [32] G. Ossola, C. G. Papadopoulos, and R. Pittau, *Nucl. Phys. B* **763**, 147 (2007); D. Forde, *Phys. Rev. D* **75**, 125019 (2007); W. T. Giele, Z. Kunszt, and K. Melnikov, *J. High Energy Phys.* 04 (2008) 049; S. D. Badger, *J. High Energy Phys.* 01 (2009) 049.
- [33] Z. Bern, L. J. Dixon, and D. A. Kosower, *Ann. Phys. (Amsterdam)* **322**, 1587 (2007); C. F. Berger and D. Forde,

- Ann. Rev. Nucl. Part. Sci.* **60**, 181 (2010); H. Ita, *J. Phys. A* **44**, 454005 (2011).
- [34] C. F. Berger, Z. Bern, L. J. Dixon, F. F. Cordero, D. Forde, T. Gleisberg, H. Ita, D. A. Kosower, and D. Maître, *Phys. Rev. Lett.* **102**, 222001 (2009).
- [35] C. F. Berger, Z. Bern, L. J. Dixon, F. F. Cordero, D. Forde, T. Gleisberg, H. Ita, D. A. Kosower, and D. Maître, *Phys. Rev. D* **80**, 074036 (2009).
- [36] C. F. Berger, Z. Bern, L. J. Dixon, F. F. Cordero, D. Forde, T. Gleisberg, H. Ita, D. A. Kosower, and D. Maître, *Phys. Rev. D* **82**, 074002 (2010).
- [37] Z. Bern, G. Diana, L. J. Dixon, F. F. Cordero, S. Höche, H. Ita, D. A. Kosower, D. Maître, and K. J. Ozeren, *Phys. Rev. D* **84**, 114002 (2011); **87**, 034026 (2013).
- [38] Z. Bern, G. Diana, L. J. Dixon, F. F. Cordero, S. Höche, D. A. Kosower, H. Ita, D. Maitre, and K. Ozeren, *Phys. Rev. Lett.* **109**, 042001 (2012).
- [39] Z. Bern, L. J. Dixon, F. F. Cordero, S. Höche, H. Ita, D. A. Kosower, N. A. L. Presti, and D. Maitre, *Phys. Rev. D* **90**, 054004 (2014).
- [40] S. D. Badger, E. W. N. Glover, and V. V. Khoze, *J. High Energy Phys.* **01** (2006) 066.
- [41] F. A. Berends and W. T. Giele, *Nucl. Phys.* **B306** (1988) 759.
- [42] H. Ita and K. Ozeren, *J. High Energy Phys.* 02 (2012) 118.
- [43] S. Catani and M. H. Seymour, *Nucl. Phys.* **B485**, 291 (1997); **B510**, 503(E) (1998).
- [44] T. Gleisberg and S. Höche, *J. High Energy Phys.* 12 (2008) 039.
- [45] T. Gleisberg, S. Höche, F. Krauss, M. Schönherr, S. Schumann, F. Siegert, and J. Winter, *J. High Energy Phys.* 02 (2009) 007.
- [46] R. Brun and F. Rademakers, *Nucl. Instrum. Methods Phys. Res., Sect. A* **389**, 81 (1997).
- [47] Z. Bern, L. J. Dixon, F. F. Cordero, S. Höche, H. Ita, D. A. Kosower, and D. Maitre, *Comput. Phys. Commun.* **185**, 1443 (2014).
- [48] G. Cullen, H. van Deurzen, N. Greiner, G. Heinrich, G. Luisoni, P. Mastrolia, E. Mirabella, G. Ossola *et al.*, *Eur. Phys. J. C* **74**, 3001 (2014).
- [49] Z. Nagy, *Phys. Rev. D* **68**, 094002 (2003).
- [50] M. Cacciari, G. P. Salam, and G. Soyez, *J. High Energy Phys.* 04 (2008) 063.
- [51] A. D. Martin, W. J. Stirling, R. S. Thorne, and G. Watt, *Eur. Phys. J. C* **63**, 189 (2009).
- [52] A. Denner, S. Dittmaier, M. Roth, and L. H. Wieders, *Nucl. Phys.* **B724**, 247 (2005); **B854**, 504 (2012).
- [53] Z. Bern, L. J. Dixon, F. Febres Cordero, S. Höche, H. Ita, D. A. Kosower, and D. Maître, *Phys. Rev. D* **92**, 014008 (2015)..
- [54] S. Frixione and B. R. Webber, *J. High Energy Phys.* 06 (2002) 029; P. Nason, *J. High Energy Phys.* 11 (2004) 040; S. Frixione, P. Nason, and C. Oleari, *J. High Energy Phys.* 11 (2007) 070; S. Alioli, P. Nason, C. Oleari, and E. Re, *J. High Energy Phys.* 06 (2010) 043; K. Hamilton and P. Nason, *J. High Energy Phys.* 06 (2010) 039; S. Höche, F. Krauss, M. Schönherr, and F. Siegert, *J. High Energy Phys.* 04 (2011) 024; 08 (2011) 123.